IEEE Photonics Journal
An IEEE Photonics Society Publication

Open Access

Grating Inscription Into Fluoride Fibers: A Review

(Invited Paper)

Volume 11, Number 5, October 2019

Alexander Fuerbach, ***Member, IEEE***
Gayathri Bharathan
Martin Ams

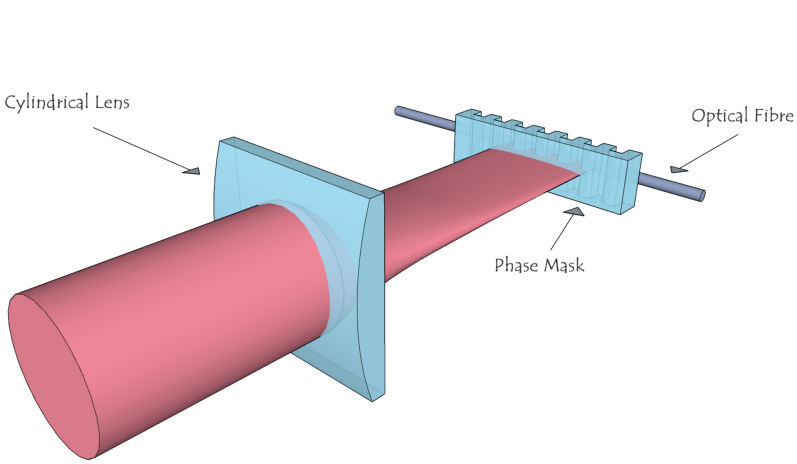

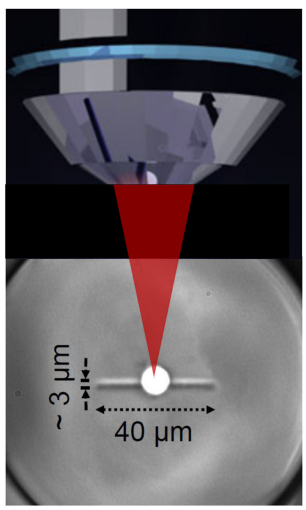

DOI: 10.1109/JPHOT.2019.2940249

IEEE photonics SOCIETY
IEEE

Grating Inscription Into Fluoride Fibers: A Review

(Invited Paper)

Alexander Fuerbach, *Member, IEEE*, Gayathri Bharathan, and Martin Ams

Department of Physics and Astronomy, MQ Photonics Research Centre, Macquarie University, Sydney, NSW 2109, Australia

DOI:10.1109/JPHOT.2019.2940249

Manuscript received July 30, 2019; revised September 2, 2019; accepted September 5, 2019. Date of publication September 9, 2019; date of current version October 2, 2019. This work was supported in part by the Air Force Office of Scientific Research under Award FA2386-16-1-4030, and in part by the OptoFab node of the Australian National Fabrication Facility, utilising NCRIS and NSW state government funding. Corresponding author: Alexander Fuerbach (e-mail: alex.fuerbach@mq.edu.au).

Abstract: First demonstrated over four decades ago, fiber gratings, and in particular fiber Bragg gratings (FBGs), have become indispensable and ubiquitous components within fiber laser cavities as well as optical communication networks and sensor systems. Because of their overwhelming use, the bulk of published work to date has concentrated on fibers that are composed of silica-based glasses, yet those become virtually opaque at wavelengths above 2 μm, i.e., in the technically increasingly important mid-infrared part of the electromagnetic spectrum. Soft glass fluoride fibers on the other hand, in particular those composed of ZBLAN (abbreviation for ZrF_4-BaF_2-LaF_3-AlF_3-NaF), offer low-loss transmission out to wavelengths of up to almost 4 μm. However, while fiber manufacturing itself has now reached a high level of maturity, with passive fiber attenuation levels as low as 1 dB/km becoming commercially available, grating fabrication in these fibers remains challenging, and research into suitable inscription techniques is still a very active and ongoing scientific field. This review aims to provide an overview of work that has been done in this area to date with an emphasis on femtosecond-laser based fabrication methods.

Index Terms: Fiber gratings, fiber Bragg gratings, Long period gratings, femtosecond laser fabrication, fluoride fibers, mid-infrared.

1. Introduction

Whenever the effective refractive index of the core of an optical fiber is modulated periodically along a section which is typically a few millimeters to several centimeters in length, a fiber grating is formed. If the physical length of a single modulation period is Λ, a wavevector with a magnitude of $\beta_G = 2\pi/\Lambda$ can be assigned to that grating. Phase matching dictates that a forward propagating core mode of wavelength

$$\lambda_{FBG} = \frac{2\, n_{eff}^{co}\, \Lambda}{m} \tag{1}$$

is coupled into a backward-propagating mode if Λ is in the order of a few microns (i.e., comparable to the wavelength), where n_{eff}^{co} is the effective index of the core mode and m is an integer representing the order of the grating [1]. In close analogy to the principle of operation of a conventional Bragg

diffraction grating, such gratings are known as a fiber Bragg gratings (FBGs) that find a vast number of applications, for example as wavelength filters [2], fiber laser mirrors [3] and optical sensors [4]. If, on the other hand, Λ is much longer than a few microns, in the order of hundreds of microns to a few millimeters, phase matching dictates that a forward propagating core mode of wavelength

$$\lambda_{LPG} = \Lambda \left(n_{eff}^{co} - n_{eff}^{cl} \right) \tag{2}$$

is coupled into a forward propagating cladding mode, where n_{eff}^{cl} is the effective refractive index of a particular cladding mode. Such a grating is therefore known as a long period grating (LPG) [5]. LPGs find applications, amongst others, as gain equalizing elements in erbium-doped fiber amplifiers [6] and in fiber-optic sensor systems [7].

Although technically not a fiber Bragg grating as per the definition above, a structure known as a 45° tilted fiber Bragg grating (TFBG) is formed if the grating planes of an FBG are tilted 45° with respect to the fiber axis. In such structures, *s* - polarized forward propagating core modes of certain wavelengths are coupled into a radiation mode (i.e., are escaping the fiber) while *p* – polarized core modes of the same wavelength remain virtually unaffected. 45° TFBGs therefore find applications as in-fiber polarizers that feature relatively broadband and highly polarization dependent dips in their transmission spectrum. The exact shape of the spectrum of a 45° TFBG can be calculated by the Green's function method as has been shown by Zhou *et al.* [8].

The first experimental demonstration of an "in-fiber reflection filter" (i.e., what is now known as a fiber Bragg grating) was achieved in 1978 in a low-mode-number germanium-doped-core silica fiber by Hill *et al.* [2]. In that seminal experiment, an argon ion laser was used to create a periodic interference pattern along the length of the fiber. After about 10 minutes of exposure, a strong grating was formed inside the core, and a reflectivity of about 88% was measured at the Bragg wavelength of 488 nm. The relatively large photosensitivity of silica fibers that enabled Hill *et al.* do fabricate the first FBG still remains the main underlying mechanism for the fabrication of commercial FBGs in similar fibers, in particular for telecommunications applications, i.e., at near-infrared wavelengths around 1550 nm.

The mid-infrared (mid-IR) part of the electromagnetic spectrum ($\approx$2.5–20 μm) is attracting significant scientific and technological interest due to the fact that virtually all molecules have their rotational or vibrational absorption lines in this wavelength range [9]. For this reason, the mid-IR is often referred to as the 'molecular fingerprint' region. Owing to the high-impact applications that directly result from these strong molecule-photon interactions, mid-IR photonics and in particular the development of coherent mid-IR sources has become one of the hottest topics in modern optics research [10]. Potential applications include, but are not limited to, environmental monitoring, trace molecular detection (e.g., for airport security screening) as well as non-invasive breath analysis and early cancer detection [11]. While different wavelengths are quoted in the literature as to where the "near-infrared" ends and the "mid-infrared" starts, a practically definition is to choose the wavelength where the use of silica-based fibers becomes impractical due to the onset of excessive transmission losses which is at about 2.5 μm. For the important class of fiber lasers that operate at wavelengths around 2.8 μm (with erbium being the laser-active ion), 2.9 μm (homium), 3.0 μm (dysprosium) or 3.5 μm (again erbium), glasses that are composed of heavier elements and that therefore feature lower phonon energies must be used. While the phonon energy of a single silicon – oxygen bond is 1100 cm^{-1}, that of a zirconium – fluoride bond is as low as 565 cm^{-1} [12]. Therefore, the fluorozirconate glass ZBLAN (abbreviation for ZrF_4-BaF_2-LaF_3-AlF_3-NaF) is the most commonly utilized material for operation between 2.5–4 μm and passive ZBLAN fibers with a loss minimum approaching 1dB/km are now becoming commercially available [13]. However, in the context of grating fabrication, it was shown that the fluorozirconates are virtually non-photosensitive [14], [15], and the established grating inscription technology based on ultraviolet (UV)-laser interference can therefore not be readily transferred from the near- to the mid-infrared. Instead, alternative fabrication methods have to be found and utilized. One approach that has been suggested in the literature is doping the ZBLAN glass matrix with the rare-earth element cerium to artificially induce a larger degree of photosensitivity. Taunay *et al.* were the first to report an UV-induced permanent

refractive index change (of the order of 10^{-5}) in a cerium-doped ZBLAN fiber [16]. However, due to the relatively low index modulation, the corresponding peak reflectivity was limited to about 10%. A substantially higher index variation of 3×10^{-4} with a correspondingly higher reflectivity of 95% was reported in a ZBLALi (ZrF,-BaF,-LaF,-AlF,-LiF) glass fiber. However, preform fabrication of the core glass required high quenching rates due to the very high concentration of cerium (5 weight %) that was required to achieve such a high index change [17]. More recently, Saad *et al.* have used a 248 nm excimer laser to inscribe FBGs into a cerium/thulium co-doped ZBLAN fiber [18]. Although the photosensitivity of the fiber was estimated to be about 50 times lower compared to standard hydrogen-loaded silica telecommunication fiber, a maximum reflectivity of 96% could be obtained.

Despite those impressive demonstrations, the most successful technology to fabricate high-quality gratings into fluoride fibers to date is to use near-infrared femtosecond laser pulses to induce a refractive index change that is not initiated by linear absorption of the photon energy, but by nonlinear ionization processes like multiphoton or tunnel ionization [19]. In a landmark paper that was published in 1996, Davis *et al.* demonstrated the feasibility of using laser pulses with a duration of 120 fs and a center wavelength of 810 nm to induce a permanent and highly localized refractive index change in silica, borate, soda lime silicate, and fluorozirconate glasses [20]. This paved the way for the afterwards rapidly expanding field of femtosecond laser direct-writing [21] and also provided the basis for the fabrication of fiber gratings into virtually any type of fibers, independent of their geometry, material or photosensitivity.

In the following section, we discuss the origin of the observed negative refractive index change in ZBLAN fibers upon irradiation with femtosecond laser pulses. In section 3, we then introduce the three main femtosecond laser-based grating inscription methods, i.e., the phase mask technique as well as the point-by-point and the line-by-line (or plane-by-plane) technique. In section 4 we provide an overview of results that have been obtained by various groups by these methods before ending with a conclusion and outlook section.

2. Femtosecond Laser Induced Refractive Index Change in ZBLAN

It is remarkable that the first publication that initially introduced the concept of inscribing optical waveguides into bulk glasses with a femtosecond laser already included ZBLAN glass in the original study [20]. However, no detailed explanations of the physical origins of the observed index change were given at the time. It was only in 2013 that Bérubé *et al.* [22] and Gross *et al.* [23] provided a much more detailed insight into the physics of the refractive index modification process. Bérubé *et al.* investigated the response of zirconium fluoride glasses with different compositions to irradiation with femtosecond pulses at low to moderate repetition rates. They found that largely independent on the exact composition of the glass, the dominant result is an observed decrease of the refractive index with a Δn in the order of 10^{-3}. For repetition rates of the inscription laser below 50 kHz, they speculated that the underlying mechanism were structural modifications due to local expansion of the irradiated region accompanied by stress-induced compression of the surrounding unexposed areas. For higher repetition rates, they observed clear signs of heat accumulation [24] and identified a very narrow process window that would allow for a smooth positive refractive index change. However, this was not confirmed by Gross *et al.* who used Raman microscopy to study the material response to irradiation with 5 MHz laser pulses. Even at such high repletion rates, a smooth and negative refractive index change with a Δn of around 10^{-3} was found. From minuscule changes in the Raman spectrum of the femtosecond laser-irradiated glass region compared to the pristine glass they were able to confirm the assumption of Berube *et al.* and concluded that the laser pulses cause local melting of the glass network followed by rapid quenching, resulting in breaking of bridging bonds between neighboring zirconium fluoride polyhedra as the glass resolidifies. As a consequence, a larger fraction of single bridging fluorine bonds relative to double bridging links are formed in comparison to the unexposed glass. Because the distance between adjacent zirconium cations is larger for single bridging than double bridging links, an expansion of the glass network and a corresponding decrease in physical and therefore also in the optical density occurs.

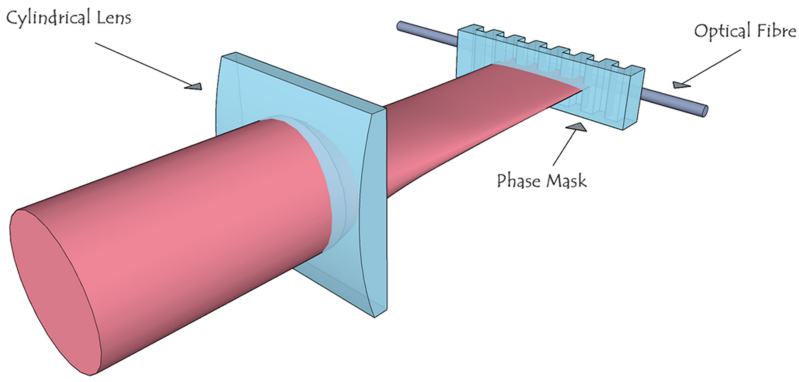

Fig. 1. Schematic of the phase mask inscription method.

3. Femtosecond Laser Based Grating Inscription Techniques

The most straightforward way to inscribe gratings into the core of an optical fiber is the use of a dedicated phase mask. In this method, a cylindrical lens is first used to produce a line focus, and a phase mask then splits the inscription laser beam mainly into the $+1$ and -1 order that interfere within the core of the optical fiber to generate the desired grating pattern as schematically shown in Fig. 1. The first experimental demonstration of gratings inscribed by this method was published by Mihailov *et al.* in 2003 who used a standard telecom silica fiber for their work [25]. While the physical length of the phase mask typically limits the total grating length to only a few millimeters, it was later also shown that by simultaneously translating the phase mask and the fiber with respect to the inscription beam, gratings with a total length that is only limited by the travel range of the translation stage used (i.e., potentially tens of centimeters) could be written [26]. The term "phase mask scanning method" was coined for this variant of the phase-mask inscription technique. While the quality of gratings fabricated with the help of a phase mask is generally very high, the main drawbacks are the typically relatively low damage threshold of the phase mask that limits the available inscription energy due to the close proximity of the phase mask to the fiber and, more importantly, the need of a dedicated phase mask for each individual grating design which makes the method relatively expensive and inflexible.

In contrast, the point-by-point (PbP) method is a highly flexible method for the fabrication of gratings with an arbitrary period that can also be varied along the length of the fiber, e.g., for the fabrication of chirped gratings. As the name suggests, in PbP gratings, a single laser pulse normally induces a single type-II damage modification [27] within the core of the fiber. As the fiber is translated relative to the inscription laser with a speed v that is equivalent to the desired period Λ of the grating multiplied by the repetition rate f of the laser (i.e., $v = \Lambda \times f$), a periodic grating pattern is formed. The first demonstrations of PbP FBGs inscribed with a femtosecond laser were reported almost simultaneously by Martinez *et al.* [28] and Wikszak *et al.* [29] in silica fibers. It was later shown that the morphology of a single grating period fabricated in this way consist of a laser-induced microvoid that is surrounded by a densified shell [30].

The strength of an FBG at a given Bragg wavelength λ_B is usually described by the so-called coupling coefficient κ that depends on the magnitude of the induced refractive index modulation (Δn) and on the mode overlap factor η as per

$$\kappa = \frac{\pi \Delta n \eta}{\lambda_B}. \tag{3}$$

The mode overlap factor is the fraction of the guided optical mode field power that propagates within the physical cross section of the FBG's refractive index perturbation. While in a PbP grating, the physical dimensions of the inscribed structures are very small (usually sub-micron diameter void-voxels), and η is therefore relatively low, the index contrast Δn is very large - basically the

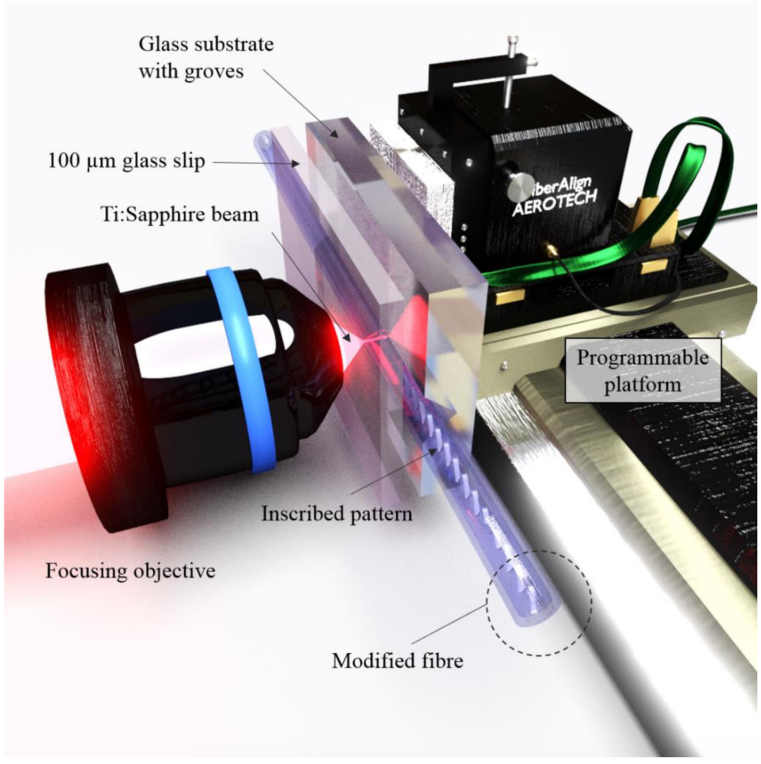

Fig. 2. Typical line-by-line (also plane-by-plane) inscription setup.

difference between the refractive index of the core glass material, typically $n_{\text{Glass}} \approx 1.5$ and the void, $n_{\text{Void}} \approx 1$. This explains how gratings with a transmission dip of as high as 60 dB can be inscribed with this method into single-mode silica fibers over short lengths of only a few millimeters.

The main drawback of the PbP method is the relatively high level of scattering losses that are a result of Mie scattering off the individual grating voxels [31]. Williams *et al.* have therefore introduced a different fabrication approach that they named "continuous core-scanning technique". Here, the writing intensity was kept below the damage threshold of the material and thus smooth type-I index modifications were inscribed into the core of the fiber instead of type-II damage modifications, resulting in a significantly reduced Δn. To compensate for this, the fiber was now also scanned transverse to the fiber axis (in addition to the translation in direction of the fiber axis) using an oscillating piezo actuator, resulting in a significantly increased mode overlap factor η. As a consequence, κ could still be kept very high, while scattering losses could be virtually eliminated [32]. However, in order to achieve a smooth index modification, in the continuous core-scanning technique the fiber has to be translated much slower as compared to the PbP technique which causes a corresponding increase in fabrication time – typically less than a minute for a PbP grating compared to several hours for a continuous core-scanned grating at a repetition rate of the inscription laser of 1 kHz. Later, Antipov *et al.* have further improved the original core-scanning technique. In their work, the fiber was placed inside a groove that was picosecond laser-machined into a glass substrate in order to keep the fiber perfectly straight over a few centimeters in length. This assembly was subsequently mounted onto a programmable 3-D air-bearing translation stage for grating inscription, see Fig. 2. This allowed full flexibility of the laser-inscribed pattern and thus perfectly parallel grating planes could be fabricated [33]. In contrast to the continuous core-scanning technique, a significantly reduced coupling to cladding modes was achieved by this true line-by-line inscription approach. Fig. 3. provides an overview of these three different fabrication methods and shows Differential Interference Contrast (DIC) images of the resulting grating patterns within the core of an optical fiber.

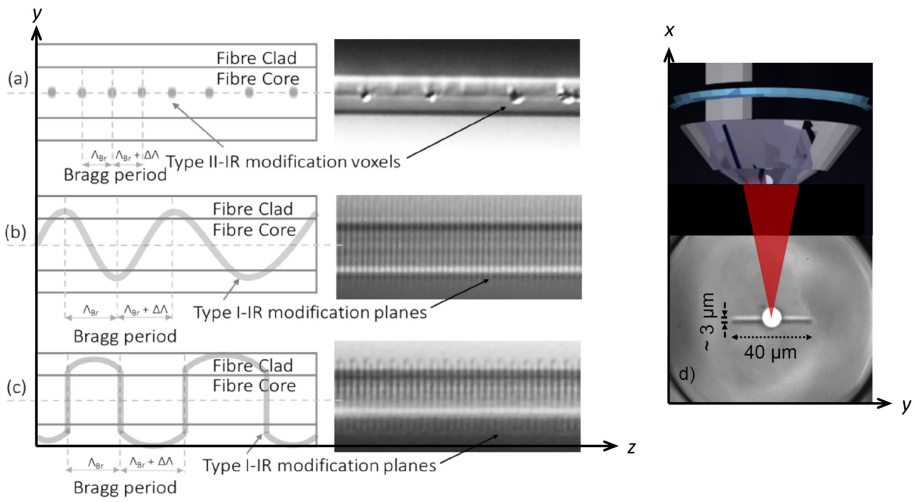

Fig. 3. Schematic representation and Differential Interference Contrast (DIC) images of different direct-write methods. (a) Point-by-point, (b) continuous core-scanning and (c) line-by-line technique. In (d), a cross-sectional view of the fiber containing a line-by-line modification is shown, highlighting the direction of the inscription beam.

While the individual lines can be inscribed across the entire core of the optical fiber (i.e., in the *y*-direction, which is in a direction that is perpendicular to both the fiber axis and to the writing beam as defined in Fig. 3.), depending on the focusing geometry, the modifications might not cover the entire cross section of the core in the direction of the writing beam (i.e., in the *x*-direction, which is in a direction that is perpendicular to the fiber axis but parallel to the writing beam as defined in Fig. 3.). The fiber axis is collinear to the *z*-direction in this case. In other words, the thickness of the inscribed lines can be smaller than the diameter of the core. In this case, the overlap factor η can be increased by stacking individual modification lines, i.e., by inscribing two (or more) lines that are slightly offset in *x*-direction at the same *z*-position. This technique is sometimes referred to as plane-by-plane inscription in the literature [34].

4. Experimental Demonstrations

4.1 Phase Mask Technique

The first demonstration of a grating that was inscribed into a fluoride fiber was reported by Bernier *et al.* in 2007 [35]. In this work, they used the phase-mask technique to inscribe a series of ≈5 mm long gratings at near infrared wavelengths into thulium-doped and undoped ZBLAN fibers using 800 nm femtosecond pulses at a repetition rate of 1 kHz. The induced refractive index change was found to be negative with a magnitude of about 10^{-3}, in agreement with previous investigations [22], [23]. The initial grating strength of 17 dB was reduced by about 50% after annealing the grating for 30 minutes at up to 125°C. The polymer coating of the fiber was removed prior to inscribing the FBG. Using the same technique, the same group later also inscribed a grating into a highly erbium-doped double-clad ZBLAN fiber at a Bragg wavelength of 2.822 μm [36]. After annealing, the reflectivity of the grating was indirectly measured to be as high as 95% and the transmission loss for light at non-resonant wavelengths was determined to be in the order of 5%. Using this FBG as the high-reflecting resonator end mirror and utilizing Fresnel reflection from the opposite end of the fiber as the output coupler, continuous-wave (cw) laser operation at 2.8 μm with an optical-to-optical conversion efficiency of 32% and an output power as high as 5 W was obtained. Later, Faucher *et al.* used a slightly different approach. In their work, the grating was also inscribed with the help of a phase-mask, yet into a section of undoped, but mode-matched double-clad fiber that was subsequently spliced onto the active fiber [37]. In this case, the grating

strength was substantially higher and the reflectivity after thermal annealing was measured to be 99.4% at 2.825 μm. Utilizing the same active fiber as in [36], the slope efficiency could be increased to 35.4% with respect to the absorbed pump power and an output power in excess of 20 W could be obtained in a passively cooled configuration. Later, the same group optimized this erbium fiber laser system further, by also inscribing a low-reflective (R $\approx$ 15%) FBG into the output end of the erbium-doped fiber, instead of utilizing only Fresnel reflection as before. To ensure spectral overlap between the two FBGs, the 2 cm long high reflecting grating (that was again inscribed into mode-matched passive fiber) was broadband, i.e., chirped at a chirp rate of 2.4 nm/cm, resulting in a reflective bandwidth of 6 nm with R $\geq$ 99%. In this configuration, a record output power of 30.5 W in continuous wave operation was obtained [38]. Further power scaling to 42 W was demonstrated later, when two FBGs with respective reflectivity of $\geq$99.5% and 8% were written directly in the core of the erbium fiber without prior removing of the protective jacket [39].

Very recently, Maes *at al.* also adopted a very similar approach to access the 3.55 μm transition in erbium via dual pumping [40]. In this work, the high-reflectivity FBG was unchirped and narrow-band and had a peak reflectivity of 90% at 3.552 μm with measured losses of less than 5% at this wavelength and with losses of around 10% at the core-pumping wavelength of 1.976 μm. In this design, the low-reflectivity output-coupling FBG was chirped to ensure spectral overlap. It had a reflectivity of $\sim$30% at 3.552 μm, a bandwidth of about 5 nm with similar loss values as compared to the high-reflective grating. Enabled by the ability to inscribe tailored FBGs into various erbium-doped ZBLAN fibers, Aydin *et al.* also demonstrated that the slope efficiency for emission at 2.8 μm can exceed the Stokes limit and can reach values of up to 50% if the two adjacent transitions of the erbium ion that correspond to emission at 2.8 μm and 1.6 μm, respectively, are cascaded [41]. To achieve this, the erbium fluoride fiber laser cavity consisted of a highly reflective input FBG with a reflectivity of $\geq$99.5% centered at 2.825 μm and Fresnel reflection on the opposite side was utilized to couple the mid-infrared light out. The collinear 1.6 μm cavity was formed by a dichroic mirror that was directly deposited on the butt-coupled silica pump fiber with a reflectivity of $\sim$80% at 1.6 μm and less than 10% at 2.8 μm, and a high reflecting FBG with a reflectivity of $\geq$99.5% at 1.614 μm that was inscribed at the opposite (output) end. This work is a great example of how advances in mid-infrared fiber laser technology can be enabled by research into the inscription of FBGs into fluoride fibers.

The possibility of utilizing the phase-mask technique also for the inscription of more complex grating designs such as π-shifted uniform FBGs has been demonstrated by dithering the phase-mask during inscription which allowed for the demonstration of a single-frequency distributed feedback (DFB) fiber laser at 2.8 μm [42].

In addition to the continuous-wave experiments described above, phase-mask written in-fiber FBGs were also reported to aid pulsed operation in fluoride fiber lasers. Paradis *et al.* recently reported a gain-switched all-fiber laser emitting at 2.8 μm with an average output power in excess of 11 W. Two individual FBGs were again inscribed with the aid of a phase mask into the opposite ends of the fiber at a Bragg wavelength of 2.826 μm. Their spectral widths and reflectivities were 0.6 nm/90% for the high reflectivity FBG and 2.2 nm/5% for the low reflectivity (output-coupling) FBG [43]. It is important to note that in this work the gratings were inscribed directly through the protective coating, i.e., without removing the coating prior to inscription in order to preserve the integrity and the robustness of the pristine fiber. Finally, Haboucha *et al.* also demonstrated the use of fiber Bragg gratings to stabilize the operation of a passively mode-locked 2.8 μm erbium fluoride glass fiber laser [44]. Here, an FBG with a reflectivity of 84% and a bandwidth of 2 nm was inscribed, and it was subsequently shown that the introduction of wavelength-selective feedback into the cavity could improve the stability of the mode-locked regime.

4.2 Direct Inscription

The first point-by-point (PbP) grating that was inscribed into a fluoride fibre was reported by Hudson *et al.* in 2013 [45]. A 20 mm long, first-order grating at a Bragg wavelength of 2.9 μm (corresponding to $\Lambda = 986$ nm) was inscribed into a holmium/praseodymium co-doped ZBLAN

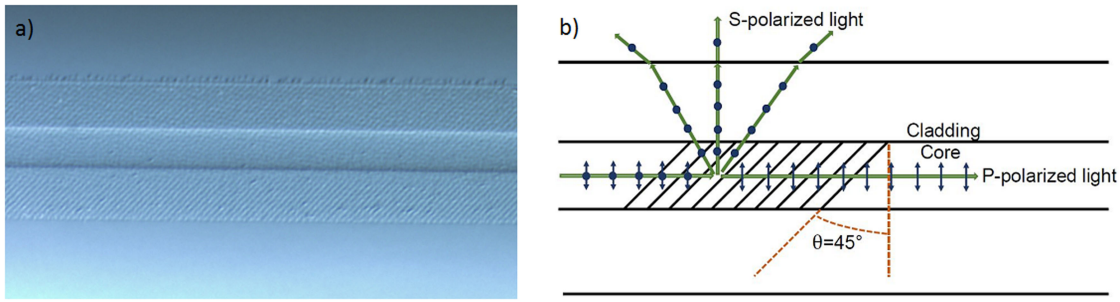

Fig. 4. (a) DIC image of a 45° tilted fiber Bragg grating inscribed by the line-by-line technique. (b) Working principle of a 45° tilted fiber Bragg grating.

fiber. The inscription laser used was a Ti:Sapphire femtosecond laser, emitting 110 fs pulses at a center wavelength of 800 nm and a repetition rate of 1 kHz. While the fabricated grating was strong enough to enable single-frequency fiber laser operation at 2.9 μm, it was observed that in contrast to PbP gratings written in silica fibers, the femtosecond-laser inscribed structures in ZBLAN fiber did not consist of microvoids, but instead of type-I refractive index modifications. It is believed that this is caused by the much lower melting temperature of ZBLAN and the softness of this glass compared to silica, which prohibits the formation of microvoids surrounded by a "frozen-in" shell of densified material during resolidification of the glass matrix. It was therefore concluded at the time that a line-by-line approach should be the more suitable technique for the fabrication of direct-written FBGs in fluoride fibers.

However, it was not until 2017, when Bharathan *et al.* demonstrated the feasibility of inscribing strong FBGs into fluoride fibers using the line-by-line method [46]. In this work, a 15 mm long second-order grating at a Bragg wavelength of 2880 nm ($\Lambda = 1.97$ μm) was inscribed into a holmium-praseodymium co-doped double clad ZBLAN fiber with a core diameter of 13 μm. The reflectivity of the grating was estimated to be 50% and utilizing the Fresnel reflection from the opposite end of the fiber as the output coupler, an all-fiber laser with a slope efficiency of 17% was realized. It was also shown that these line-by-line gratings could be inscribed directly though the outer polymer coating of the fiber, without the need of removing the coating before inscription. Therefore, the strength of the already relative brittle fluoride fiber was not compromised during grating inscription and stress-strain tuning of the grating could be utilized to sweep the lasing wavelength over a tuning rage of as large as 37 nm.

The extraordinary flexibility of the line-by-line technique was demonstrated by the same group shortly after by inscribing a 16 mm long 45° tilted FBG into the same active ZBLAN fiber. Fig. 4(a) shows a DIC image of the fabricated structure. As the induced refractive index change is $\ll 1 (\approx 10^{-3})$, each inscribed line acts as a Brewster-plate due to

$$\Theta_B = arctan\frac{n_2}{n_1} = arctan\frac{n_{Core} + \Delta n}{n_{Core}} \approx \arctan(1) = 45^\circ, \tag{4}$$

as schematically shown in Fig. 4(b). Such fabricated in-fiber polarizer transformed an initially completely unpolarized fiber laser operating at 2.9 μm into a linear polarized laser with a 21.6 dB output polarization extinction ratio (PER) [47]. The assumption that very low loss values could be achieved with type-I line-by-line gratings was confirmed by the fact that the unpolarized laser and the laser with the 45° tilted FBG inscribed exhibited almost identical slope efficiencies.

A non-tilted line-by-line FBG was later also inscribed into a single-clad dysprosium-doped ZBLAN fiber. The 17 mm long second-order FBG with $\Lambda = 2.12$ μm yielded a reflection of about 60% at 3.15 μm which enabled the realization of a Watt-level dysprosium fiber laser at 3.15 μm with a record-high slope efficiency of 73% [48].

While all of the gratings inscribed by the line-by-line technique as discussed above were written at second order to avoid overlap between adjacent grating planes, Goya *et al.* recently reported the

fabrication of a 2.5 mm long first-order FBG for a Bragg wavelength of 2800 nm (corresponding to $\Lambda = 0.947$ μm) with a reported reflectivity of 97% [49]. This was achieved by utilizing a femtosecond inscription laser with a shorter wavelength (532 nm compared to 800 nm) and by using an objective lens with a very high numerical aperture (NA) of 1.4. To ensure that the overlap factor η was large, despite the very small focal spot, a plane-by-plane approach was used. The grating was inscribed into a double-clad erbium-doped ZBLAN fiber and used as the high reflective end mirror in a fiber laser, with Fresnel reflection from the opposite end acting as the output coupler. In this work, Goya *et al.* also monitored the lasing evolution in-situ during FBG inscription and found that the peak lasing wavelength begins to shift from a free-running (and unstable) peak towards the Bragg wavelength λ_{FBG} once the grating exceeds a length of only L = 0.3 mm. Beyond L = 0.62 mm, the peak wavelength become stable at the Bragg wavelength.

In order to investigate the influence of the writing parameters on the strength of the fabricated gratings, Bharathan *et al.* recently performed a systematic study into the inscription of line-by-line gratings into passive ZBLAN fibers [50]. This work led to several important conclusions: First, it was shown that a change in translation speed and/or in the energy of the femtosecond laser pulses during inscription cannot be used to tune the reflectivity of the fabricated gratings. It was concluded that only a very narrow parameter window in terms of translation speed and pulse energy could be utilized for the inscription of FBGs of any kind, in stark contrast to silica fibers where lower pulse energies and higher translation speeds typically result in the formation of weaker gratings. Further, it was shown that overpassing, i.e., inscribing the same line twice per grating period, does not lead to an increase in Δn, and thus also not to an increase in κ. Stacking on the other hand (i.e., plane-by-plane writing) was shown to be an efficient way to increase the reflectivity of a grating. In this work, FBGs with the highest coupling coefficients of any directly written gratings into fluoride fibers (as high as 464 m^{-1}) and record low losses ($<$0.5 dB/cm) could be demonstrated after a meticulous optimization of the inscription process. In this work, it was finally shown for the first time that thermal annealing of line-by-line grating at 150 °C for about 6 hours results in a blue shift of the Bragg wavelength as well as in a significant increase in grating strength (in contrast to a decrease as reported in phase-mask written gratings). There is some evidence that this could be caused by a selective migration of zirconium and hafnium ions during annealing, yet further studies are required [51].

Finally, very recently *Heck at al.* have inscribed a long-period grating into erbium-doped double clad ZBLAN fiber [50]. In this work, the focusing conditions were optimized such that the laser focus covered almost the entire cross section of the core of the fiber that was then translated in direction of the fiber axis (i.e., not transverse to the fiber axis as during line-by-line inscription). This was done at a slow enough speed to inscribe a continuous modification in direction of the fiber axis. The laser power was modulated by a mechanical shutter at a 50% duty cycle to realize a periodic modulation with $\Lambda = 100$ μm over a total length of 75 mm. By using an inscription laser with a high repetition rate of 250 kHz, heat accumulation effects in the focal volume could be utilized and attenuation peaks with a magnitude of up to 24 dB could be obtained. Interestingly, thermal annealing in this case resulted in a significant reduction in grating strength and a slight red shift of the grating resonance. Shortly after, the same group demonstrated that these LPGs could be used for the mitigation of parasitic laser effects in mid-infrared fiber amplifiers [53].

5. Conclusions and Outlook

The mid-infrared part of the electromagnetic spectrum is emerging as a crucial and enabling tool for many applications due to the strong and highly specific absorption of molecules in this range. The fabrication of mid-infrared compatible fibers is now reaching a level of maturity and reproducibility that is a prerequisite for the widespread use of this technology. What is still lacking behind is the development of fiber-coupled or fiber-integrated optical components. Recently, there have been advances in the fabrication of broadband and wavelength-dependent couplers for the mid-infrared, based on chalcogenide optical fibers [54] and splicing methods to join silica pump fibers and actively doped fluoride fibers are constantly improving [55], [56]. Also, there is active research into the development of mid-infrared integrated components that can potentially be coupled to fluoride

optical fibers [57], [58]. The capability of fabricating high-quality fiber gratings, in particular fiber Bragg gratings into fluoride fibers remains one of the key challenges that will enable mid-infrared fiber technology to transition out of the lab and into practical applications. Femtosecond-laser inscription of these gratings, either via the use of phase masks or via line-by-line direct inscription is emerging as the most promising technology for this task. Fiber Bragg gratings, 45° tilted fiber Bragg gratings as well as long period gratings with properties that closely match their near-infrared silica fiber counterparts can now readily be produced in fluoride fibers. However, further research is required to make the fabrication process more reproducible, and in particular into understanding the role of ion-migration in the refractive index modification process and in the thermal annealing properties of these gratings.

Acknowledgments

The authors would like to thank R. Williams for useful discussions.

References

[1] R. Kashyap, *Fiber Bragg Gratings*. New York, NY, USA: Academic, 1999.
[2] K. O. Hill, Y. Fujii, D. C. Johnson, and B. S. Kawasaki, "Photosensitivity in optical fiber waveguides: Application to reflection filter fabrication," *Appl. Phys. Lett.*, vol. 32, no. 10, pp. 647–649, 1978.
[3] S. Pradhan, G. E. Town, and K. J. Grant, "Dual-wavelength DBR fiber laser," *IEEE Photon. Technol. Lett.*, vol. 18, no. 16, pp. 1741–1743, Aug. 2006.
[4] W. W. Morey, G. Meltz, and W. H. Glenn, "Fiber optic Bragg grating sensors," *Proc. SPIE*, vol. 1169, pp. 98–107, 1990.
[5] A. M. Vengsarkar, P. J. Lemaire, J. B. Judkins, V. Bhatia, T. Erdogan, and J. E. Sipe, "Long-period fiber Bragg gratings as band-rejection filters," *J. Lightw. Technol.*, vol. 14, no. 1, pp. 58–65, Feb. 1996.
[6] M. Harurnoto, M. Shigehara, and H. Suganuma, "Gain-flattening filter using long-period fiber gratings," *J. Lightw. Technol.*, vol. 20, no. 6, pp. 1027–1033, Jun. 2002.
[7] V. Bhatia and A. M. Vengsarkar, "Optical fiber long-period grating sensors," *Opt. Lett.*, vol. 21, no. 9, pp. 692–694, 1996.
[8] K. Zhou, G. Simpson, X. Chen, L. Zhang, and I. Bennion, "High extinction ratio in-fiber polarizers based on 45° tilted fiber Bragg gratings," *Opt. Lett.*, vol. 30, no. 11, pp. 1285–1287, 2005.
[9] J. S. Li, W. Chen, and H. Fischer, "Quantum cascade laser spectrometry techniques: A new trend in atmospheric chemistry," *Appl. Spectrosc. Rev.*, vol. 48, no. 7, pp. 523–559, 2013.
[10] "Nature photonics focus issue: Mid-infrared photonics," *Nature Photon.*, vol. 6, no. 7, pp. 407–498, 2012.
[11] A. B. Seddon *et al.*, "Prospective on using fibre mid-infrared supercontinuum laser sources for in vivo spectral discrimination of disease," *Analyst*, vol. 143, pp. 5874–5887, 2018.
[12] S. D. Jackson, "Towards high-power mid-infrared emission from a fibre laser," *Nature Photon.*, vol. 6, pp. 423–431, 2012.
[13] 2019. [Online]. Available: https://leverrefluore.com/products/passive-fibers/
[14] M. Zeller, T. Lasser, H. G. Limberger, and G. Mazé, "UV-Induced index changes in undoped fluoride glass," *J. Lightw. Technol.*, vol. 23, no. 2, pp. 624–627, Feb. 2005.
[15] G. M. Williams, T. E. Tsai, C. I. Merzbacher, and E. J. Friebele, "Photosensitivity of rare-earth-doped ZBLAN fluoride glasses," *J. Lightw. Technol.*, vol. 15, no. 8, pp. 1357–1362, Aug. 1997.
[16] T. Taunay *et al.*, "Ultraviolet-induced permanent Bragg gratings in cerium-doped ZBLAN glasses or optical fibers," *Opt. Lett.*, vol. 19, no. 17, pp. 1269–1271, 1994.
[17] H. Poignant *et al.*, "Efficiency and thermal behaviour of cerium-doped fluorozirconate glass fibre Bragg gratings," *Electron. Lett.*, vol. 30, no. 16, pp. 1339–1341, 1994.
[18] M. Saad, L. R. Chen, and X. Gu, "Highly reflective fiber Bragg gratings inscribed in Ce/Tm Co-doped ZBLAN fibers," *IEEE Photon. Technol. Lett.*, vol. 25, no. 11, pp. 1066–1068, Jun. 2013.
[19] A. Kaiser, B. Rethfeld, M. Vicanek, and G. Simon, "Microscopic processes in dielectrics under irradiation by subpicosecond laser pulses," *Phys. Rev. B*, vol. 61, no. 17, pp. 11437–11450, 2000.
[20] K. M. Davis, K. Miura, N. Sugimoto, and K. Hirao, "Writing waveguides in glass with a femtosecond laser," *Opt. Lett.*, vol. 21, no. 21, pp. 1729–1731, 1996.
[21] R. R. Gattas and E. Mazur, "Femtosecond laser micromachining in transparent materials," *Nature Photon.*, vol. 2, no. 4, pp. 219–225, 2008.
[22] J. P. Bérubé, M. Bernier, and R. Vallée, "Femtosecond laser-induced refractive index modifications in fluoride glass," *Opt. Mater. Exp.*, vol. 3, no. 5, pp. 598–611, 2013.
[23] S. Gross, D. G. Lancaster, H. Ebendorff-Heidepriem, T. M. Monro, A. Fuerbach, and M. J. Withford, "Femtosecond laser induced structural changes in fluorozirconate glass," *Opt. Mater. Exp.*, vol. 3, no. 5, pp. 574–583, 2013.
[24] S. M. Eaton *et al.*, "Heat accumulation effects in femtosecond laser-written waveguides with variable repetition rate," *Opt. Exp.*, vol. 13, no. 12, pp. 4708–4716, 2005.
[25] S. J. Mihailov *et al.*, "Fiber Bragg gratings made with a phase mask and 800-nm femtosecond radiation," *Opt. Lett.*, vol. 28, no. 12, pp. 995–997, 2003.
[26] J. Thomas *et al.*, "Inscription of fiber Bragg gratings with femtosecond pulses using a phase mask scanning technique," *Appl. Phys. A*, vol. 86, no. 2, pp. 153–157, 2007.

[27] S. Gross, M. Dubov, and M. J. Withford, "On the use of the type I and II scheme for classifying ultrafast laser direct-write photonics," *Opt. Exp.*, vol. 23, no. 6, pp. 7767–7770, 2015.
[28] A. Martinez, M. Dubov, I. Khrushchev, and I. Bennion, "Direct writing of fibre Bragg gratings by femtosecond laser," *Electron. Lett.*, vol. 40, no. 19, pp. 1170–1172, 2004.
[29] E. Wikszak, J. Burghoff, M. Will, S. Nolte, A. Tunnermann, and T. Gabler, "Recording of fiber Bragg gratings with femtosecond pulses using a 'point by point' technique," in *Proc. Conf. Lasers Electro-Opt.*, San Francisco, CA, USA, 2004, Paper CThM7.
[30] J. Thomas *et al.*, "Cladding mode coupling in highly localized fiber Bragg gratings: Modal properties and transmission spectra," *Opt. Exp.*, vol. 19, no. 1, pp. 325–341, 2010.
[31] M. L. Åslund *et al.*, "Optical loss mechanisms in femtosecond laser-written point-by-point fibre Bragg gratings," *Opt. Exp.*, vol. 16, no. 18, pp. 14248–14254, 2008.
[32] R. J. Williams, R. G. Krämer, S. Nolte, and M. J. Withford, "Femtosecond direct-writing of low-loss fiber Bragg gratings using a continuous core-scanning technique," *Opt. Lett.*, vol. 38, no. 11, pp. 1918–1920, 2013.
[33] S. Antipov, M. Ams, R. Williams, E. Magi, M. J. Withford, and A. Fuerbach, "Direct infrared femtosecond laser inscription of chirped fiber Bragg gratings," *Opt. Exp.*, vol. 24, no. 1, pp. 30–40, 2016.
[34] P. Lu *et al.*, "Plane-by- plane inscription of grating structures in optical fibers," *J. Lightw. Technol.*, vol. 36, no. 4, pp. 926–931, 2018.
[35] M. Bernier *et al.*, "Bragg gratings photoinduced in ZBLAN fibers by femtosecond pulses at 800 nm," *Opt. Lett.*, vol. 32, no. 5, pp. 454–456, 2007.
[36] M. Bernier, D. Faucher, N. Caron, and R. Vallée, "Highly stable and efficient erbium-doped 2.8 micron all fiber laser," *Opt. Exp.*, vol. 17, no. 19, pp. 16941–16946, 2009.
[37] D. Faucher, M. Bernier, G. Androz, N. Caron, and R. Vallée, "20 W passively cooled single-mode all-fiber laser at 2.8 μm," *Opt. Lett.*, vol. 36, no. 7, pp. 1104–1106, 2011.
[38] V. Fortin, M. Bernier, S. T. Bah, and R. Vallée, "30 W fluoride glass all-fiber laser at 2.94 μm," *Opt. Lett.*, vol. 40, no. 12, pp. 2882–2885, 2015.
[39] Y. O. Aydin, V. Fortin, R. Vallée, and M. Bernier, "Towards power scaling of 2.8 μm fiber lasers," *Opt. Lett.*, vol. 43, no. 18, pp. 4542–4545, 2018.
[40] F. Maes, V. Fortin, M. Bernier, and R. Vallée, "5.6 W monolithic fiber laser at 3.55 μm," *Opt. Lett.*, vol. 42, no. 11, pp. 2054–2057, 2017.
[41] Y. O. Aydın *et al.*, "Diode-pumped mid-infrared fiber laser with 50% slope efficiency," *Optica*, vol. 4, no. 2, pp. 235–238, 2017.
[42] M. Bernier, V. Michaud-Belleau, S. Levasseur, V. Fortin, J. Genest, and R. Vallée, "All-fiber DFB laser operating at 2.8 μm," *Opt. Lett.*, vol. 40, no. 1, pp. 81–84, 2015.
[43] P. Paradis, V. Fortin, Y. O. Aydin, R. Vallée, and M. Bernier, "10 W-level gain-switched all-fiber laser at 2.8 μm," *Opt. Lett.*, vol. 43, no. 13, pp. 3196–3199, 2018.
[44] A. Haboucha, V. Fortin, M. Bernier, J. Genest, Y. Messaddeq, and R. Vallée, "Fiber Bragg grating stabilization of a passively mode-locked 2.8 μm Er^{3+}: Fluoride glass fiber laser," *Opt. Lett.*, vol. 39, no. 11, pp. 3294–3297, 2014.
[45] D. D. Hudson, R. J. Williams, M. J. Withford, and S. D. Jackson, "Single-frequency fiber laser operating at 2.9 μm," *Opt. Lett.*, vol. 38, no. 14, pp. 2388–2390, 2013.
[46] G. Bharathan, R. I. Woodward, M. Ams, D. D. Hudson, S. D. Jackson, and A. Fuerbach, "Direct inscription of Bragg gratings into coated fluoride fibers for widely tunable and robust mid-infrared lasers," *Opt. Exp.*, vol. 25, no. 24, pp. 30013–30019, 2017.
[47] G. Bharathan, D. D. Hudson, R. I. Woodward, S. D. Jackson, and A. Fuerbach, "In-fiber polarizer based on a 45-degree tilted fluoride fiber Bragg grating for mid-infrared fiber laser technology," *OSA Continuum*, vol. 1, no. 1, pp. 56–63, 2018.
[48] R. I. Woodward, M. R. Majewski, G. Bharathan, D. D. Hudson, A. Fuerbach, and S. D. Jackson, "Watt-level dysprosium fiber laser at 3.15 μm with 73% slope efficiency," *Opt. Lett.*, vol. 43, no. 7, pp. 1471–1474, 2018.
[49] K. Goya *et al.*, "Plane-by-plane femtosecond laser inscription of first-order fiber Bragg gratings in fluoride glass fiber for in situ monitoring of lasing evolution," *Opt. Exp.*, vol. 26, no. 25, pp. 33305–33313, 2018.
[50] G. Bharathan, T. T. Fernandez, M. Ams, R. I. Woodward, D. D. Hudson, and A. Fuerbach, "Optimized laser-written ZBLAN fiber Bragg gratings with high reflectivity and low loss," *Opt. Lett.*, vol. 44, no. 2, pp. 423–426, 2019.
[51] A. Fuerbach, G. Bharathan, T. T. Fernandez, and M. Ams, "Fabrication of gratings in mid-infrared compatible fibres via femtosecond laser direct inscription," in *Proc. Int. Conf. Transparent Opt. Netw.*, Angers, France, 2019, Paper We.D6.4.
[52] M. Heck, S. Nolte, A. Tünnermann, R. Vallée, and M. Bernier, "Femtosecond-written long-period gratings in fluoride fibers," *Opt. Lett.*, vol. 43, no. 9, pp. 1994–1997, 2018.
[53] M. Heck, J. C. Gauthier, A. Tünnermann, R. Vallée, S. Nolte, and M. Bernier, "Long period fiber gratings for the mitigation of parasitic laser effects in mid-infrared fiber amplifiers," *Opt. Exp.*, vol. 27, no. 15, pp. 21347–21357, 2019.
[54] F. Tavakoli, A. Rekik, and M. Rochette, "Broadband and wavelength-dependent chalcogenide optical fiber couplers," *IEEE Photon. Technol. Lett.*, vol. 29, no. 9, pp. 735–738, May 2017.
[55] M. M. Kozak, W. Kowalsky, and R. Caspary, "Low-loss glue splicing method to join silica and fluoride fibres," *Electron. Lett.*, vol. 41, no. 16, pp. 897–899, 2005.
[56] K. Yin, B. Zhang, J. Yao, L. Yang, S. Chen, and J. Hou, "Highly stable, monolithic, single-mode mid-infrared super-continuum source based on low-loss fusion spliced silica and fluoride fibers," *Opt. Lett.*, vol. 41, no. 5, pp. 946–949, 2016.
[57] J. M. Morris *et al.*, "$Ge_{22}As_{20}Se_{58}$ glass ultrafast laser inscribed waveguides for mid-IR integrated optics," *Opt. Mater. Exp.*, vol. 8, no. 4, pp. 1001–1011, 2018.
[58] M. R. Vázquez *et al.*, "Femtosecond laser inscription of nonlinear photonic circuits in gallium lanthanum sulphide glass," *J. Phys., Photon.*, vol. 1, no. 1, 2019, Art. no. 015006.